IEEE Access
Multidisciplinary ⋮ Rapid Review ⋮ Open Access Journal

Received February 23, 2022, accepted March 22, 2022, date of publication March 31, 2022, date of current version April 11, 2022.

Digital Object Identifier 10.1109/ACCESS.2022.3163712

Recognizing Semi-Natural and Spontaneous Speech Emotions Using Deep Neural Networks

AMMAR AMJAD[1], LAL KHAN[1], NOMAN ASHRAF[2], MUHAMMAD BILAL MAHMOOD[3], AND HSIEN-TSUNG CHANG[1,4,5,6]

[1]Department of Computer Science and Information Engineering, College of Engineering, Chang Gung University, Taoyuan 33302, Taiwan
[2]CIC, Instituto Politécnico Nacional, Mexico City 7738, Mexico
[3]Department of Software Engineering, Dalian University of Technology, Dalian 116024, China
[4]Artificial Intelligence Research Center, Chang Gung University, Taoyuan 33302, Taiwan
[5]Department of Physical Medicine and Rehabilitation, Chang Gung Memorial Hospital, Taoyuan 333, Taiwan
[6]Bachelor Program in Artificial Intelligence, Chang Gung University, Taoyuan 33302, Taiwan

Corresponding author: Hsien-Tsung Chang (smallpig@widelab.org)

This work was supported by the Chang Gung Memorial Hospital under Grant CMRPD2J0023.

ABSTRACT We needed to find deep emotional features to identify emotions from audio signals. Identifying emotions in spontaneous speech is a novel and challenging subject of research. Several convolutional neural network (CNN) models were used to learn deep segment-level auditory representations of augmented Mel spectrograms. The proposed study introduces a novel technique for recognizing semi-natural and spontaneous speech emotions based on 1D (Model A) and 2D (Model B) deep convolutional neural networks (DCNNs) with two layers of long-short-term memory (LSTM). Both models used raw speech data and augmented (mid, left, right, and side) segment level Mel spectrograms to learn local and global features. The architecture of both models consists of five local feature learning blocks (LFLBs), two LSTM layers, and a fully connected layer (FCL). In addition to learning local correlations and extracting hierarchical correlations, LFLB comprises two convolutional layers and a max-pooling layer. The LSTM layer learns long-term correlations from local features. The experiments illustrated that the proposed systems perform better than conventional methods. Model A achieved an average identification accuracy of 94.78% for speaker-dependent (SD) with a raw SAVEE dataset. With the IEMOCAP database, Model A achieved an average accuracy of an SD experiment with raw audio of 73.15%. In addition, Model A obtained identification accuracies of 97.19%, 94.09%, and 53.98% on SAVEE, IEMOCAP, and BAUM-1s, the databases for speaker-dependent (SD) experiments with an augmented Mel spectrogram, respectively. In contrast, Model B achieved identification accuracy of 96.85%, 88.80%, and 48.67% on SAVEE, IEMOCAP, and the BAUM-1s database for SI experiments with augmented reality Mel spectrogram, respectively.

INDEX TERMS Speech emotion recognition, convolutional neural network, data augmentation, long-short-term memory, spontaneous speech database.

I. INTRODUCTION

Speech is an efficient, quick, and fundamental way of human communication. Speech signals are one of the most natural ways humans express their emotions. Speech emotion recognition (SER) is a challenging task in artificial intelligence, pattern recognition, signal processing, and other fields [1], [2]. The existing studies [3], [4] have been on SER problems using data gathered in laboratory-controlled conditions, such as the acted and simulated databases [5], [6] to identify emotions. Whereas semi-natural emotions are linked with high identification accuracy, these emotions can be easily exaggerated. However, acted emotions fail to accurately represent the features of human emotional expression in natural situations. Spontaneous emotions are more demanding and harder to describe than acted or semi-natural emotions in the wild. Therefore, emotion recognition in the wild has attracted much attention. Although, extracting the most discriminative features for speech expression feature extraction is essential for the SER frameworks. The fundamental emotional characteristics [7], [8] of speech are low-level descriptors (LLDs). The commonly used LLDs

The associate editor coordinating the review of this manuscript and approving it for publication was Yongming Li.

consist of prosody, voice quality, and spectral characteristics [7]–[9]. Recently, many large feature sets based on LLDs, including INTERSPEECH 2010 [10], ComParE [11], AVEC 2013 [12], and GeMAPS [13] have been proposed for SER. Handcrafted audio features are utilized as an input of neural networks when utilizing transfer learning and deep learning approaches for SER [3], [14]–[16]. The overall outcome of handcrafted features extraction from specific emotions is very high; however, the extraction of handcrafted features generally requires human effort [17], [18]. Accordingly, improved features extraction methods are required to effectively identify the most discriminative emotional features.

The newly developed deep learning methods [19], [20], which have attained significant attention in the SER, provide suitable solutions [14], [21], [22] to the problems mentioned above. Multiple deep neural frameworks have been utilized for high-level feature learning tasks, such as deep neural networks (DNNs) [23]–[25], deep convolutional neural networks (CNNs) [26], and Long short-term memory recurrent neural networks (LSTM-RNNs) [27]. DNNs comprise one or more underlying hidden layers between inputs and outputs based on feed-forward architectures. Automated feature learning approaches were developed to acquire high-level features that accurately recognize human emotions [10], [12], [13], [28], [29], and all have given better results. The DNN method was the first deep learning method deployed, correlated with handcrafted acoustic characteristics. In [30], introduced a DNN-based (Gerda) approach, following the Mahalanobis minimum-distance classifier (MDC) for SER, to learn the discriminative features of 6552 low-level acoustic descriptors (LLDs). The DNN [31] was utilized to learn high-level features from handcrafted features. Emotion classification was fostered by using an extreme learning machine (ELM) [32]–[34]. MFCCs are used as an input of DNN for obtaining high-level features. An extreme learning machine (ELM) is utilized to classify speech emotions [35]. The author in [36], utilized a DNN to compress an utterance into a fixed-length matrix by pooling the last hidden layer actions across time. Then, the encoded matrices are used to learn an ELM kernel for the utterance-level classification of speech emotions. DNNs cannot successfully acquire discriminative features for SER because DNNs typically require handcrafted characteristics as SER inputs.

CNN's are composed of multi-level convolutional and pooling layers, which allows obtaining mid-level feature representations using data input and train models. To take advantage of CNNs' outstanding performance in computer vision applications [26], 2D time-frequency representations generated from acoustic spectra are often input into CNNs for SER. Specifically, the researchers of [32] used spectrograms as input data of a hybrid network that comprises a sparse auto-encoder and a one-layer CNN to train salient features for SER. The suggested approach [37] used segment-level spectrograms as CNN input to extract discriminative characteristics. In [38], segment-level features are extracted using an image spectrogram as inputs to a deep network such as AlexNet [26]. Implementation of CNNs with LSTM-RNNs has recently been a new study topic in SER. The studies [39], [40] proposed an attention-based bidirectional LSTM with a spatial CNN for deep spectrum feature extraction by utilizing segment-level spectrograms. In [14], the proposed method used a segment-level spectrogram with a deep convolutional LSTM architecture.

Notice that the two-dimension mentioned above (2D) CNN techniques such as CNN, CNN+LSTM, and CNN+RNN, effectively extract energy modulation features. As a result, these time and frequency features, which extract 2D time and frequency spectrograms of audio data, performed very well in SER applications. Moreover, various 1D CNN models have been employed in recent years for features extraction in SER, and other applications [41]–[45]. For example, the researchers in [46] investigated the efficacy of the different 1D CNN architectures for extracting features from the 1D original waveforms on SER challenges. However, these utilized 1D CNN models with one or two convolution layers are shallow, making their learned 1D CNN features inappropriate for SER. On the other hand, 1D CNNs trained on sample-level 1D audio waveforms have been effectively used for music categorization, using feature extraction learned from the original 1D raw audio waveforms.

In [32], a sparse auto-encoder was used to learn essential features from spectrogram for SER with one-layer CNN. The end-to-end SER framework with a combination of two-layers CNN with an LSTM is presented in [33], [34]. A recurrent neural network (RNN) is designed to handle long-range dependencies [47]. In suggested techniques [3], [32]–[34], researchers used limited data from publically available emotional speech databases to develop deep CNNs with one or two convolutional layers (CL). In [15], [48] found that varying lengths of spectrogram yield different affective cues for recognizing specific emotions because other emotions dominated separate segment-level features in an utterance. Therefore, when various segment features are used for speech emotion recognition, the discriminating strength of the retrieved utterance-level features changes for an utterance. This study proposed a new spontaneous and semi-natural SER approach based on the deep CNN+LSTM architecture. Similar to [14], [49], the proposed approach used multiple image scales as inputs to a single CNN. This approach is different from other approaches, so-called multiscale systems [50] in which CNN's use with subnetwork is based on specific information. To further increase SER performance, we integrate deep LFLB with LSTM at different lengths of RGB spectrograms. The presented approach learns local features from raw audio spectrograms using deep CNNs on target publically available databases. Then, to achieve utterance-level feature extraction for SER, the temporal dynamic information is modeled using an LSTM. Experiments were performed on two semi-natural datasets and one spontaneous emotional speech dataset (BAUM-1s) [51].

The main contributions of this research are as follows:

- Considering the augmented Mel spectrogram presents various emotional signals for recognizing certain emotions, this proposed study used a multiscale system for semi-natural and spontaneous datasets. We believe that this is the first work in which a multiscale framework with a local feature learning block has been used for spontaneous and semi-natural datasets for SER.
- The following layers are used to extract local level features from raw and augmented data: convolutional, batch normalization (BN), exponential linear unit, and max-pooling layers in the local feature learning block (LFLB).
- Two LSTM layers are added to build networks that connect to the LFLB to learn long-term dependencies from a series of obtained features.
- For the first time, a 1D CNN+LSTM (Model A) model can learn many emotional characteristics from raw speech datasets. However, the two-dimensional CNN+LSTM models (Model B) outperform Model A in the proposed study. The Model B was designed to learn local correlations and global contextual information from an augmented Mel spectrogram. The LFLB or LSTM layers may handle the augmented Mel spectrogram as a series or grid.F

The rest of this paper is structured as follows.

The related works is given in Section 2. Details of our proposed method are given in Section 3. Results are provided in Section 4. Conclusion and future work are presented in Section 5.

II. RELATED WORKS

Distinguishing features are essential for recognizing speech emotions from audio signals. Spectrum features are among the different prosody features that are utilized in SER. AB Kandali *et al.* used the Gaussian mixture model (GMM) with MFCC to recognize emotions from the Assamese speech database [52]. VB Waghmare *et al.* used MFCCs as the main feature to identify emotions in the Marathi speech dataset [53]. After extracting MFCCs from EmoDB, Demircan, S., utilized k-NN to identify emotions [54]. Chenchah *et al.* employed HMM and SVM [55] to determine the spectral features obtained from raw speech data. In [56] proposed an SER approach with an auto-associative neural network (AANN) by fusing residual phase and MFCC features. AANN, SVM, and RBFNN are used to identify emotions in a music database using two acoustic features [57]. However, handcrafted features are highly effective for distinguishing emotions in audio data but are primarily low-level features. A generalized discriminant analysis (Gerda) deep neural network (DNN) layered with multiple limited Boltzmann machines (RBMs) was used in [30] to identify emotions. The results were significantly better than traditional baseline methods. In [58], the suggested approach used a regression-based DBN with three hidden layers to extract features and identify emotions from a music database. The proposed technique [59] investigated a hybrid approach and obtained the best outcomes on FAU Aibo. The suggested research [60] used a deep neural network to detect utterance level emotions. It achieved a 20% relative accuracy increase over conventional state-of-the-art methods. In [32], developed a semi CNN approach with a linear SVM to identify emotional classes. In [61], the suggested CNN architecture was used to identify emotions from labeled datasets, and preliminary experimental outcomes noticed that this approach performed better than SVM-based classification. In [61] proposed a systematic method for developing an effective emotion detection system utilizing deep DCNNs and annotated training data. Furthermore, [15] compressed the extracted audio features using PCA. The proposed technique is different from the work mentioned above. The developed models learn local and global features to identify emotions from audio data. In general, models are only capable of identifying low-level features. Furthermore, existing methods based on CNN can only extract a single kind of emotion-related information, which is insufficient for recognizing emotions.

In [62], authors used text and audio data from the IEMOCAP database to demonstrate a double recurrent encoder framework technique that uses MFCC with text tokens as input characteristics. The suggested multimodal approach resulted in a 71.8% accuracy on the testing dataset. In [63], the suggested model is used to train two classifiers, RNN and SVM, using the CREMA-D database for accounting for voice level variation. Three intensity levels were used to train the classifiers: low, medium, and high. The emotions labeled "happy" and "neutral" have the highest categorization accuracy, whereas the emotion labeled "disgust" has the lowest. Furthermore, they did not produce any epoch-by-epoch accuracy curves or a class-by-class confusion matrix to support their claims. Therefore, in [64] proposed the remaining block and memory attention methods and 3D LMS-based, dilated CNNs. They employed a combination of the static LMS feature, the Δ(delta), and the $\Delta\Delta$(double delta) feature to create the feature vector from raw speech. When using the speaker-dependent collection, IEMOCAP obtained 74.96% accuracy, and when using the speaker-independent raw data, it achieved 69.32% accuracy. The model obtained the best accuracy of 90.37 percent with the IEMOCAP database.

High-level information extracted from speech spectrograms is used to build an SER model proposed in [65]. It was determined how well the model performed using two different data sets. The IEMOCAP and EMO-DB datasets have an accuracy of 77.1% and precision of 92.2%, respectively. Zhang *et al.* [66] offer a novel multi-task learning approach. The RAVDESS database contains both voice and music samples with four emotional states, and the model acquired a 57.14% accuracy rate for selecting group multi-task feature sets. In [67], scientists collected and computed mean values for the 20-MFCC, the twenty delta, and the twenty double delta characteristics. Input for the artificial neural network algorithm was these mean values. Using the EMO-DB and RAVDESS datasets, they obtained 82.3 percent and 87.8%

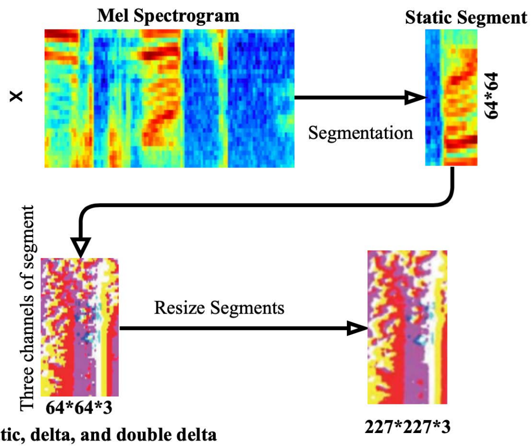

FIGURE 1. The process of generating three channels using Mel spectrogram segments.

accuracy with their approach. Badshah *et al.*proposed an SER design for a 2D CNN-based model based on the EMO-DB database [68]. A pre-trained AlexNet [69] design was also used, but the results were dismal. They also looked into transfer learning. The first suggested model had an accuracy rate of 84.3% on the test set. Previous research has shown that ensemble approaches may improve speech recognition accuracy [70]–[72] in SER tasks.

III. PROPOSED METHOD

One of the primary objectives of SER is to extract more discriminative emotional features from raw audio and augmented data. Emotional features are divided into two types: handcrafted features and deep learning features. Many handcrafted feature extraction approaches are developed carefully with ingenious strategies. Most deep learning approaches [30], [48], [73]–[75] are used to extract deep learning features from speech emotional datasets and perform well for SER. Therefore, identifying emotions using deep learning features is becoming more popular. Raw databases, environments, and discriminative features are the main concerns for SER. The proposed approach is divided into three sections: (1) preparation of the raw data, (2) learning local and global features, and (3) the architecture of Model A and Model B.

A. PREPARATION OF THE RAW DATA

The initial step is to generate a suitable input for LFLB. For this purpose, we created different lengths of Mel spectrogram segments. The generated Mel spectrogram segments have a fixed input size $(227 * 227 * 3)$. As stated in [4], we generate three channels of spectrogram segments. These spectrogram segments are identical to the RGB format of the original 1D audio signals. We created 2D Mel spectrogram segments of size $(Mel_{spectrogram} = W * S)$ for an utterance. S represents the total number of Mel filter banks (MFB), and W is the context window size. We used $(S = 64)$ to calculate the Mel spectrogram with a 25ms window size and a 10 ms overlap [14]. Then we use a contextual window of W frames to divide the Mel spectrogram into $(64 * W)$ segments. In [76], the used $250 - ms$ audio clip may provide information about emotions. This result indicates that W is greater than and equal to 23 and that its segment length is 245 milliseconds. Delta (Δ) and Double Delta $(\Delta\Delta)$ coefficients are generally obtained from MFCCs in speaker recognition to represent the spatio-temporal in auditory segments. Also, first and second-order spectrogram regression coefficients of $Mel_{spectrogram}$ calculated using their corresponding spectrogram slice' (Δ) coefficients and $(\Delta\Delta)$ coefficients. As a result, we can get three channels of Mel spectrogram slices with a scale of $(64 * W * 3)$. The obtained Mel spectrogram is identical to the RGB image. The bilinear interpolation is used to resize various Mel spectrogram slices into a suitable size $(227 * 227 * 3)$ as input for LFLB to recognize features of the obtained channels of the Mel spectrogram slices. The process for generating three channels of Mel spectrogram segment slices (static, delta, and double delta) used as inputs to LFLB is shown in Figure 1. Semantic information was not included in the auditory Mel spectrogram segments. As a result, obtained features are inputted into deep learning models to generate segment features. $(W = 64)$ in [4], [14] was utilized as the primary SER function. This research aims to determine the effect of various subgroup length W inputs on frameworks. The detailed description of datasets is illustrated in Table 1, and Table 2 shows the structure of databases.

B. DEEP FEATURE LEARNING

A novel approach for learning local and global level discriminative features from raw audio databases and augmented Mel spectrograms is presented in our study. We combined an LSTM and LFLB to learn local level and global level features. The CL of LFLB processed a grid of values G [77]–[79]. The LFLB is used to learn a feature sequence and each feature in a sequence is a function of a limited number of input features. Whereas LSTM is used for processing the G-series of numbers [47], every element of the learning features is a function of the preceding output elements. The high-level features can be learned using a combination of the CNN+LSTM approach. The CNN+LSTM method contains both long-term contextual dependencies and local information.

C. LOCAL FEATURE LEARNING

LFLB extracts emotional features from the input signal. As shown in Figure 2, LFLB consists of five layers. 1) two convolutional layers (CL), 2) batch normalization layer (BNL) [80], 3) exponential linear unit (ELU), and 4) max-pooling layer (MPL). The first, second, and fourth are the core layers of LFLB. The main advantages of the CL are spatial locality and shared weights [77]–[79]. However, spatial locality and shared weights enable CL's learning kernel capability. At each batch, BN normalized the activation function of the CL and enhanced the stability and performance of the deep neural network. Deep neural networks

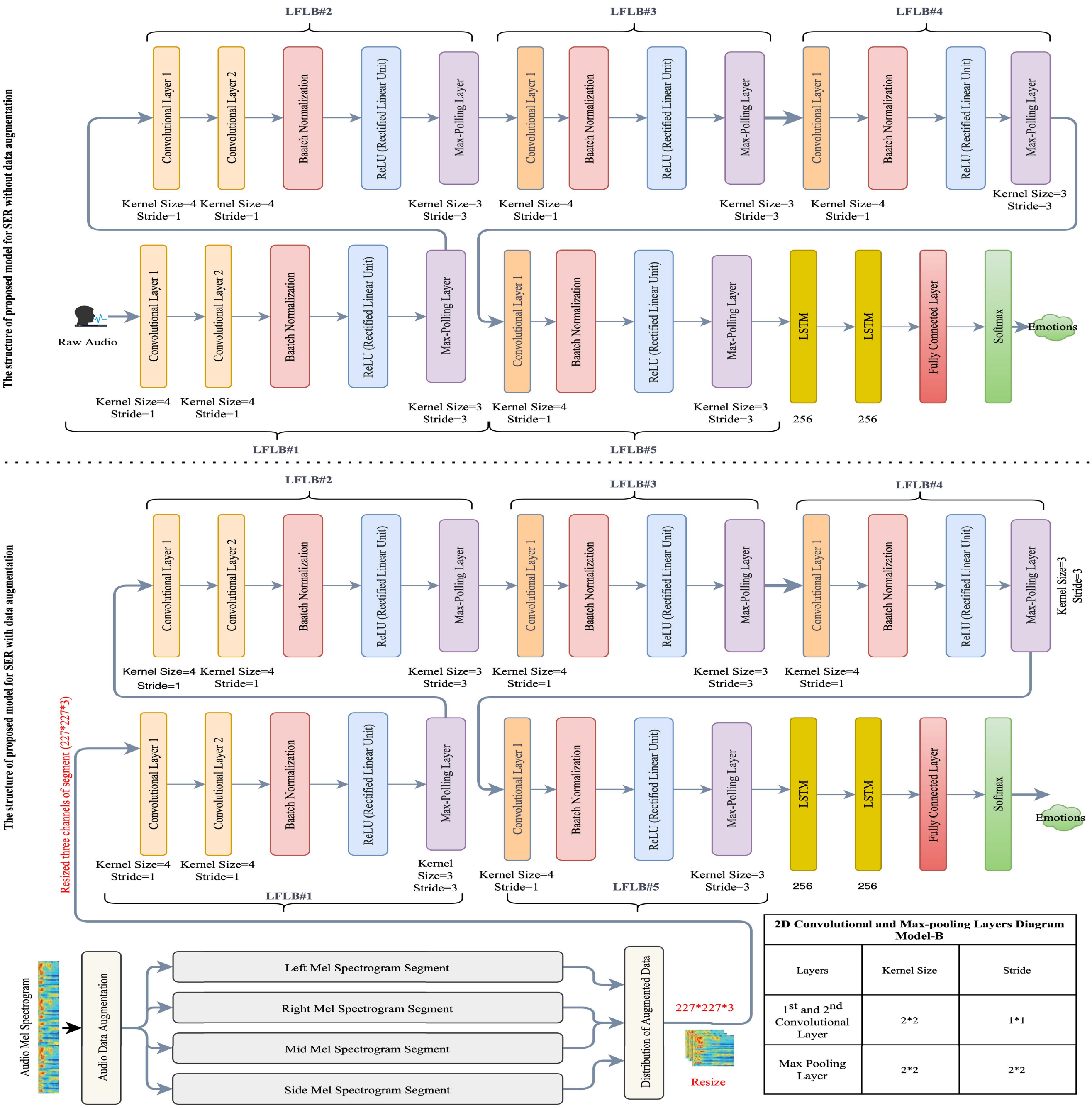
The structure of proposed model for SER without data augmentation
LFLB#1
LFLB#2
LFLB#3
LFLB#4
LFLB#5
Raw Audio
Convolutional Layer 1
Convolutional Layer 2
Baatch Normalization
ReLU (Rectified Linear Unit)
Max-Polling Layer
Kernel Size=4 Stride=1
Kernel Size=3 Stride=3
LSTM
256
Fully Connected Layer
Softmax
Emotions
The structure of proposed model for SER with data augmentation
Resized three channels of segment (227*227*3)
Audio Mel Spectrogram
Audio Data Augmentation
Left Mel Spectrogram Segment
Right Mel Spectrogram Segment
Mid Mel Spectrogram Segment
Side Mel Spectrogram Segment
Distribution of Augmented Data
227*227*3
Resize

2D Convolutional and Max-pooling Layers Diagram Model-B

Layers	Kernel Size	Stride
1st and 2nd Convolutional Layer	2*2	1*1
Max Pooling Layer	2*2	2*2

FIGURE 2. The structure of proposed model for SER.

perform better and are more stable when using BN layers. It is possible to keep the mean activation near zero and the activation standard deviation close to one by using batch normalization [81]. The ELU determines the output of the BN layer. Although ELU has negative values in contrast to other activation functions, in the suggested approach, ELU speeds up the learning process and leads to better identification accuracy [82]. By using a PL, the extracted features can be more robust against distortion and noise. The most common non-linear function is max-pooling, which divides the input into on-overlapping groups and returns the highest value for each sub-group [83].

The LFLB can be customized in various ways, depending on the task. The modification in the LFLB is generally reflected in the various convolution and max-pooling parameters. A local feature extractor is performed by the convolution layer. The data convolved over the height and width of the input value using the kernels. When convolved features pass into the CL, we can obtain a feature map by computing the dot product of the input and kernel elements. Suppose a signal

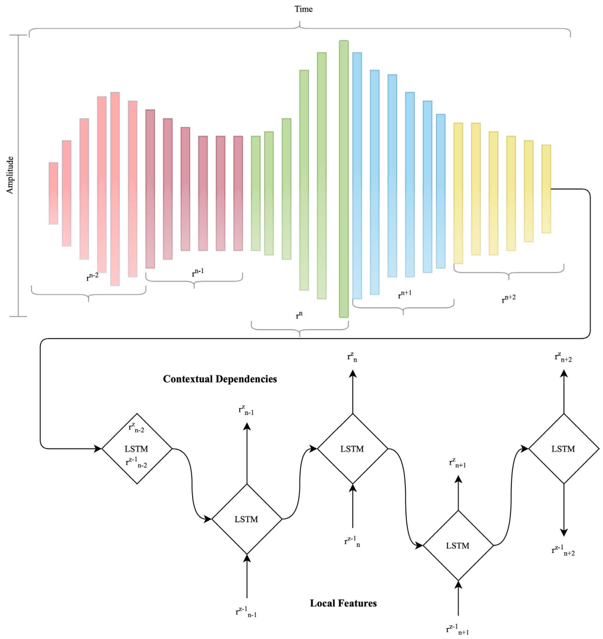

FIGURE 3. Top Figure: Description of one-dimensional local features learning block from audio samples (the colors represent various active forms of the learning block). Bottom Figure: LSTM learning of contextual dependencies from local descriptors.

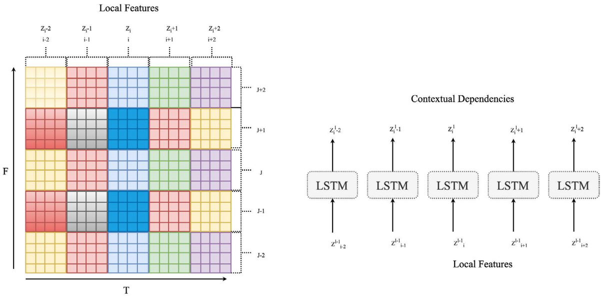

FIGURE 4. Two-dimensional convolution and pooling diagrams.

$s(n)$ is fed into a 1D CL. Convolution of the signal $s(n)$ with the kernel $k(n)$ and the size of the kernel z yields the output $r(n)$. We randomly initialized the proposed approach to the 1D convolution kernel $k(n)$.

$$r(n) = s(n) * k(n) = \Sigma_{m=-z}^{z} s(m).k(n-m) \tag{1}$$

If $s(x, y)$ is the input of the 2D CL, the result $r(x, y)$ is achieved by convolving a signal $s(x, y)$ with the convolution kernel $k(x, y)$, and size is $i * j$. In the proposed approach, we randomly initialized the 2D convolution kernel k.

$$\begin{aligned} r(x*y) &= s(x*y) * k(x*y) \\ &= \Sigma_{i=-a}^{a} \Sigma_{j=-b}^{b} s(i,j).k(x-i, y-j) \end{aligned} \tag{2}$$

The convolved features fed into BN normalized the activation function of preceding layers in every batch. The second layer of LFLB uses a transformation to maintain the mean constant. In the case of the convolved features, the variance is 1. When correlated features are input into the third layer of LFLB, output features are explained as below:

$$r_x^z = \sigma(BN(b_x^z + \Sigma_y r_y^{z-1} * k_{xy}^z)) \tag{3}$$

where r_x^z and r_y^{z-1} defines the x output and y input features at the z layer and $z-1$ layer, in the above equation, k_{xy}^z represents the convolution kernel between the x and y features. The BN (.) correlated with the learning features of the CL. In the proposed study, the ELU activation function is represented by the function $\sigma(h)$, which can be written as:

$$\sigma(h) = \left\{ \begin{matrix} h \quad h \geq 0 \\ \alpha(ev^h - 1), h < 0 \end{matrix} \right\} \tag{4}$$

Suppose the value of α is greater than zero and ev is Euler's value. In that case, output features are inputted into the MPL. The PL is used for non-linear down-sampling functionality, decreasing feature resolution. The extracted features obtained by the max-pooling layer are as follows:

$$r_q^z = max_{\forall w \in \Omega_q} r_w^z \tag{5}$$

In eq. (5),Ω_q indicates the pooling value with the value of the index k, and r_q^z and r_w^z defines the input and output features of the MPL with index q and w.

D. GLOBAL FEATURES LEARNING

The architecture of LSTM is the same as a recurrent neural network (RNN) [47], [84]. LSTM specifically understands long-term dependencies from series of segments. So it is stacked upon the LFLB used to learn contextual dependencies from the sequences of extracted local level features. Because LSTM uses four components to modify the block state: an input gate, an output gate, a forget gate, and a self-recurrent cell. Equations (6)-(10) [84] depict the upgrading of an LSTM unit at each time step. Let zp be the input volume and zq be the output volume of an LSTM network. The correlation between zp and zq can be written as:

$$\begin{aligned} a^t &= \sigma_p(G_a z_t^{x-1} + H_a z_t^{x-1} + k_a) && (6) \\ e^t &= \sigma_p(G_e z_e^{x-1} + H_e z_t^{x-1} + k_e) && (7) \\ r^o &= \sigma_p(G_r z_t^{x-1} + H_r z_t^{x-1} + k_r) && (8) \\ o_t &= f_t \cdot o_{t-1} + i_t \cdot \sigma_o(G_o z_t^{x-1} + H_o z_t^{x-1} + k_o) && (9) \\ m_t^x &= o_t \cdot \sigma_m z_t && (10) \end{aligned}$$

where ot is the LSTM unit state; G, H, and k denote parameter matrices and vectors; a_t, e_t, and r_t denote gate vectors; p denotes a sigmoid function; σ_m and. σ_o is the hyperbolic tangent; The (.) operator represented the Hadamard product. In equations (6)–(10), the input and output feature indices are superscripts $x - 1$ and l. The variables a, e, and r in the equations above represent the forget, input, and output gate. In eq. (9), o represent a cell value. The variable p in the above equations represents the gate.

TABLE 1. Detailed description of datasets.

Datasets	Speakers	Emotions	Languages	Size	Avg. samples of each emotion per person
SAVEE	4 (male)	Seven emotions (sadness, neutral, frustration, happiness, disgust ,anger, surprise)	480 utterances (120 utterances per speaker)British English	480 utterances (120 utterances per speaker)	15
IEMOCAP	10 (5 Male, 5 Female)	Nine emotions (surprise, happiness, sadness, anger, fear, excitement, neutral, frustration and others)	English	12 Hours Recording	100.3
BAUM-1s [51]	31 (13Male, 18 Female)	Six emotions (anger, joy, sadness, disgust, fear, surprise)	unscripted and unguided way in Turkish	1222 video sample	

TABLE 2. Original SAVEE, IEMOCAP and BAUM-1s databases structure.

Datasets	Sad	Angry	Happy	Disgust	Neutral	Surprise	Frustration	Excited	Joy	Fear
SAVEE	60	60	60	60	120	60	–	–	–	60
IEMOCAP	1182	1229	495	4	575	24	3830	2505	–	135
BAUM-1s	139	56	179	86	187	43	22(Boredom)	–	64	38

TABLE 3. The Model A parameters are as follows: The output is determined by the length and number. In Learning Block 1, the CL is represented by *C* while the max-pooling layer is represented by *P*.

Name		OutputDim	Size of Kernel	Stride
Learning Block 1	C1st and C2nd	L*128	4	1
Learning Block 1	P 1st	L/4*128	3	3
Learning Block 2	C 3rd and C4th	L/4*128	4	1
Learning Block 2	P 2nd	L/16*128	3	3
Learning Block 3	C 5th	L/16*256	4	1
Learning Block 3	P 3rd	L/64*256	3	3
Learning Block 4	C 6th	L/64*256	4	1
Learning Block 4	P 4th	L/256*256	3	3
Learning Block 5	C 7th	L/256*512	4	1
Learning Block 5	P 5th	L/512*512	3	3

E. ARCHITECTURE OF MODEL A

As shown in Figure 2, the architecture of Model A consists of five LFLBs, and each LFLB block consists of five layers. We apply the following rules to distinguish between different layers: 1) The number before the label specifies the network in which the building block or layer is located. 2) The number after the label specifies the index number of the layer in a network. Figure 2 depicts the general architecture of the proposed model. Model A is based on a deep learning method that learns from raw datasets. Consequently, in each LFLB, the convolution and pooling layers are one-dimensional. The kernel size for the first and second blocks is 128; for the third and fourth blocks, it is 256. The kernel size and stride of all the max-pooling layers is three. Model A's parameters are illustrated in Table 3, and softmax is the last layer of Model A used to recognize emotions.

Next, a one-dimensional vector representing an audio clip is inputted into Model A, where LFLBs learn local features. After being reshaped, the output features from the five one-dimensional learning blocks are given to the LSTM layers. Finally, the contextual dependencies are identified from the inputted local hierarchical properties. Figure 3 illustrates the local level extracted features and contextual dependencies. So, the output of the LSTM layers comprises local and long-term contextual dependencies. Next, output features are inputted into FCL, followed by two LSTM layers. Below is the equation for the FCL:

$$s^l = b^l + s^{l-1}.kl \tag{11}$$

The softmax layer is used as a classifier. The softmax layer makes predictions based on the input features. The Softmax function is described as follows:

$$z_i = \Sigma_j h_j W_{ji} \tag{12}$$

$$softmax(z)_i = p_i = \frac{e^{z_i}}{\Sigma_{j=1}^{n} e^{z_i}} \tag{13}$$

where softmax input is Z_i, W_{ij} is the weight, and h_j is the activation function. So, the predicted class label $\hat{u}$ represented as:

$$\hat{u} = argmaxp_i \tag{14}$$

F. ARCHITECTURE OF MODEL B

The architecture of Model B is similar to that of Model A. As shown in Figure 2, Model B consists of five LFLBs,

TABLE 4. The parameters for Model B are shown in the table below, and output is specified by height * width * digit, where M indicates the low-level features. In 2D LFLB, convolutional and maximum pooling layers are denoted as C1st and P1st, respectively.

Name		OutputDim	Size of Kernel	Stride
Learning Block 1	C 1st and C2nd	M*N*64	2*2	1*1
Learning Block1	P 1st	M/2*N/2*64	2*2	2*2
Learning Block 2	C 3rd and C 4th	M/2*N/2*64	2*2	1*1
Learning Block 2	P 2nd	M/8*N/8*64	2*2	2*2
Learning Block 3	C 5^{5h}	M/8*N/8*128	2*2	1*1
Learning Block 3	P 3rd	M/32*N/32*128	3*3	3*3
Learning Block 4	C 6th	M/32*N/32*128	2*2	1*1
Learning Block 4	P 4th	M/128*N/128*128	3*3	3*3
Learning Block 5	C 7th	M/128*N/128*128	2*2	1*1
Learning Block 5	P 5th	M/128*N/128*128	3*3	3*3

TABLE 5. The comparison of classification accuracies of Model A and Model B.

Database	Type	Raw audio data	Augumented Mel spectrogram
		Accuracy of SD Experiments	
SAVEE dataset	Semi-Natural	94.78	97.19
IEMOCAP dataset	Semi-Natural	73.15	94.09
BAUM-1s dataset	Spontaneous	31.61	53.98
		Accuracy of SI Experiments	
SAVEE dataset	Semi-Natural	87.54	96.85
IEMOCAP dataset	Semi-Natural	69.53	88.80
BAUM-1s dataset	Spontaneous	29.10	48.67

TABLE 6. The average classification accuracy of Model B was compared to that of other feature extraction and classification models using the SAVEE database.

Research work	Accuracy of SD	Accuracy of SI
[3]	82.10	66.90
[74]	88.3	85.2
[75]	–	92.9
[85]	75.5	–
[86])	91.6	85.8
Our Work	97.19	96.85

TABLE 7. Comparison of Model B recognition accuracy with various feature extraction approaches and classification methods using the IEMOCAP dataset.

Research work	Accuracy of SD	Accuracy of SI
[3]	83.80	76.60
[61]	91.6	85.8
[73]	88.3	85.2
[64]	74.96	69.32
Our Work	94.09	88.80

TABLE 8. The average classification accuracy of Model B was compared to that of other feature extraction and classification models using the BAUM-1s database.

Research work	Model Accuracy
[14]	45.27
[15]	44.31
[59]	45.60
Our Work	48.67

two LSTM layers, and one FCL with 2D convolution and pooling. The kernels in the first two LFLBs are 64, and the rest are 128. The size of the kernel and stride in the first and second LFLBs is 2*2 and 1*1, respectively. The kernel and size for the pooling layers are 2*2 for the first two blocks; for the rest, it's 3*3. Table 4 illustrates the parameters of model B. The softmax is used as a classifier in Model B. Keras [87] was used to implement both models. Model B is used to learn high-level features from the Mel spectrogram. Five LFLBs/s learn local features with local correlations from an augmented Mel spectrogram. The output features from LFLB5 are resampled into a temporal sequence and used as input for the first LSTM layer. Local features are used to learn contextual dependencies. Figure 4 depicts the learning of local-level features and contextual dependencies. As a result, the LSTM layer's output comprises spatial correlations and global contextual information. The FCL is used to categorize these features into the output space. Softmax is used for classification using learned features.

G. HYPERPARAMETER OPTIMIZATION

It is crucial to select hyperparameters for a neural network before moving further. Hyperparameter optimization aims to maximize a deep neural network's efficiency on a database independent of the deep neural network under evaluation. Confusion matrix, arbitrary search, and other search strategies were all effectively used in various deep learning models. They all help improve the training of the deep model. The Bayesian optimization technique produces higher performance with fewer testing datasets. [88]–[90]. The Bayesian optimization technique is used in our studies to choose hyperparameters for suggested DNNs. Bayesian optimization is a sequential design approach that effectively solves the optimization problem. In our studies, we utilized Hyperopt to maximize the hyperparameters [90]. Hyperopt provides a

TABLE 9. Recognition accuracy of Mid Mel spectrogram techniques.

Types	BAUM-1s		IEMOCAP		SAVEE	
	SD	SI	SD	SI	SD	SI
Mid	42.40	36.88	75.78	70.98	77.64	79.09

minimizer-friendly optimal solution and analyzes it like a randomized function. The goal function is also given prior knowledge. The probability distributions over the optimization problem are modified following the collected function evaluations. Using probability distributions, we may generate an acquired function. Recursively, hyperparameters were chosen. As a first step in selecting an optimization technique, a distribution over the variables is chosen (adagrad, Adam, SGD, and RMS). The proposed design is presented once the learning with optimal parameters has been performed.

IV. RESULTS

The proposed models' performance was evaluated using semi-natural and spontaneous databases for SD and SI experiments. In addition, we evaluated our models using two experiments. The first experiment was performed using raw audio samples, and the second was performed using an augmented Mel spectrogram. Model A is used to extract features from raw audio samples in the presented study. In contrast, Model B extracts high-level features from augmented Mel spectrogram.

Additionally, the developed models are used for predictive capacity instead of limited explanatory power. Numerous methods are presented to reduce the possibility of overfitting in proposed studies. Overfitting is a factor in bad predictions for untrained datasets because overfit models memorize training sets instead of learning to predict better. Although overfitting occurs for numerous reasons, (1) when the model's architecture is very complicated, (2) Overfitting occurs when a learning model becomes overtrained. (3) when the model degrees of freedom are too high [91]. Many techniques have been developed to minimize overfitting, including regularization [92], BN [81], cross-validation [93], early stopping [93], and model-selection [94].

A. SPEAKER DEPENDENT (SD) EXPERIMENTS

First, we performed SD experiments on both augmented Mel spectrogram and raw audio speech signals. The datasets were randomly divided into an 80:20 ratio for training and testing. Our experiment results imply that the proposed models efficiently identify speech emotions. The main goal of the proposed study is to identify emotions with high accuracy and generalization performance. Therefore, the best-predicted model is reported in our experiments. Figure 5 illustrates the results achieved from the SAVEE database for SD experiments. Model B recognized "neutral", "angry", "frustration", and "sad" with the highest accuracies of 100%, 97.58%, 97.43%, and 97.12% respectively, with the SAVEE dataset with raw audio data. While Model B achieved the average accuracy of 97.19% with an augmented Mel spectrogram. As shown in Figure 6, the SAVEE database identified "anger" and "sad" with the highest accuracy of 100%. At the same time, "disgust," "surprise," and "neutral" were recognized with the highest accuracies of 98.66%, 98.13%, and 96.48% with the SAVEE datasets of an augmented Mel spectrogram, respectively. Model B recognized "frustration", "happy", and" anger" with the accuracies of 51.07%,47.66%, and 45.20% with the IEMOCAP dataset of a raw audio dataset, as illustrated in Figure 7. Figure 8 illustrates the IEMOCAP dataset contains four emotions," sad", "anger", "happy", and "neutral", which are listed with accuracies of 97.28%, 94.66%,56.66%, and 89.37%, with an augmented Mel spectrogram, respectively. Model B achieved 69.53% and 85.34% average accuracy with raw audio and augmented Mel spectrogram for the IEMOCAP database, respectively. As shown in Figure 9, the BAUM-1s database identified "joy" with the highest accuracy

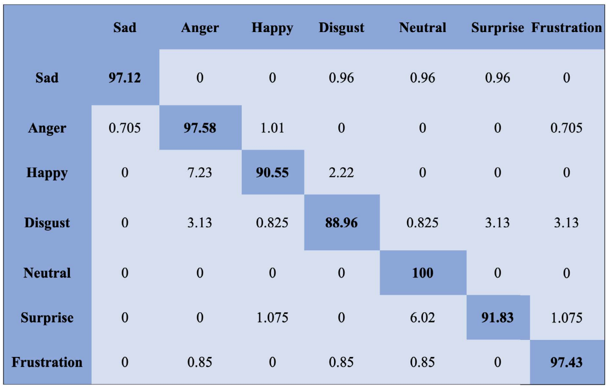

	Sad	Anger	Happy	Disgust	Neutral	Surprise	Frustration
Sad	**97.12**	0	0	0.96	0.96	0.96	0
Anger	0.705	**97.58**	1.01	0	0	0	0.705
Happy	0	7.23	**90.55**	2.22	0	0	0
Disgust	0	3.13	0.825	**88.96**	0.825	3.13	3.13
Neutral	0	0	0	0	**100**	0	0
Surprise	0	0	1.075	0	6.02	**91.83**	1.075
Frustration	0	0.85	0	0.85	0.85	0	**97.43**

FIGURE 5. The confusion matrix of SD experiments on the SAVEE dataset of raw audio data.

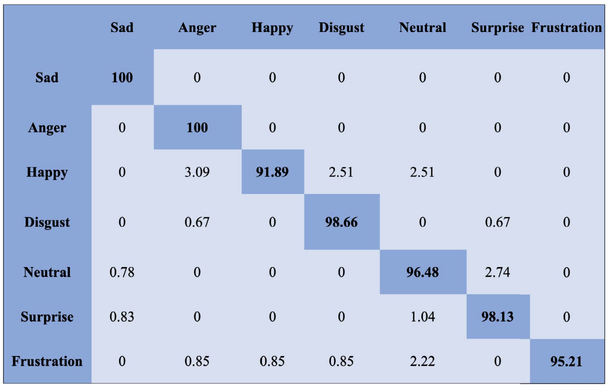

	Sad	Anger	Happy	Disgust	Neutral	Surprise	Frustration
Sad	**100**	0	0	0	0	0	0
Anger	0	**100**	0	0	0	0	0
Happy	0	3.09	**91.89**	2.51	2.51	0	0
Disgust	0	0.67	0	**98.66**	0	0.67	0
Neutral	0.78	0	0	0	**96.48**	2.74	0
Surprise	0.83	0	0	0	1.04	**98.13**	0
Frustration	0	0.85	0.85	0.85	2.22	0	**95.21**

FIGURE 6. The confusion matrix of SD experiments on SAVEE dataset of augmented Mel spectrogram.

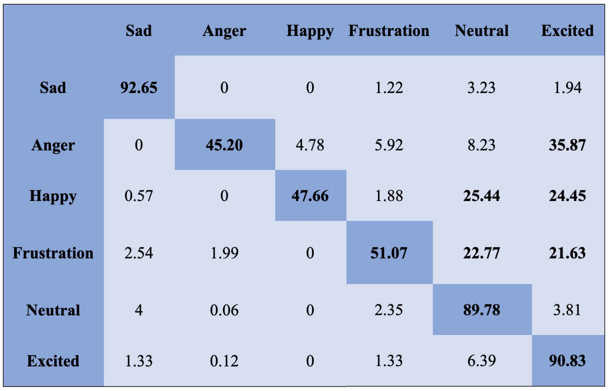

	Sad	Anger	Happy	Frustration	Neutral	Excited
Sad	92.65	0	0	1.22	3.23	1.94
Anger	0	45.20	4.78	5.92	8.23	35.87
Happy	0.57	0	47.66	1.88	25.44	24.45
Frustration	2.54	1.99	0	51.07	22.77	21.63
Neutral	4	0.06	0	2.35	89.78	3.81
Excited	1.33	0.12	0	1.33	6.39	90.83

FIGURE 7. The confusion matrix of SD experiments on the IEMOCAP dataset of raw audio data.

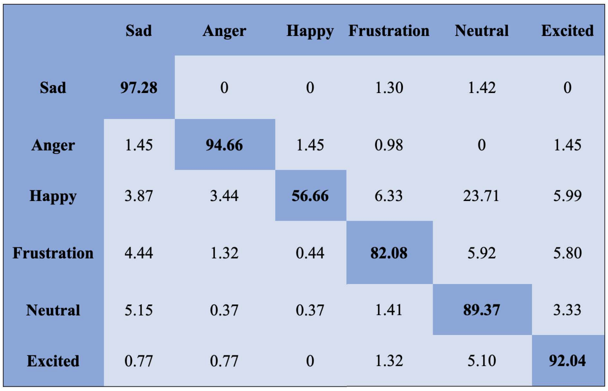

	Sad	Anger	Happy	Frustration	Neutral	Excited
Sad	97.28	0	0	1.30	1.42	0
Anger	1.45	94.66	1.45	0.98	0	1.45
Happy	3.87	3.44	56.66	6.33	23.71	5.99
Frustration	4.44	1.32	0.44	82.08	5.92	5.80
Neutral	5.15	0.37	0.37	1.41	89.37	3.33
Excited	0.77	0.77	0	1.32	5.10	92.04

FIGURE 8. The confusion matrix of SD experiments on IEMOCAP dataset of augmented Mel spectrogram.

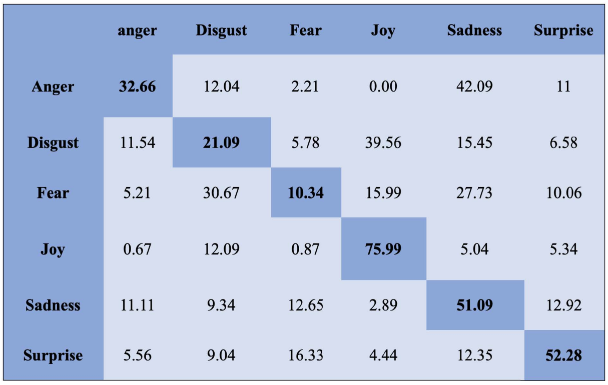

	anger	Disgust	Fear	Joy	Sadness	Surprise
Anger	32.66	12.04	2.21	0.00	42.09	11
Disgust	11.54	21.09	5.78	39.56	15.45	6.58
Fear	5.21	30.67	10.34	15.99	27.73	10.06
Joy	0.67	12.09	0.87	75.99	5.04	5.34
Sadness	11.11	9.34	12.65	2.89	51.09	12.92
Surprise	5.56	9.04	16.33	4.44	12.35	52.28

FIGURE 9. The confusion matrix of SD experiments on BAUM-1s dataset of raw audio dataset.

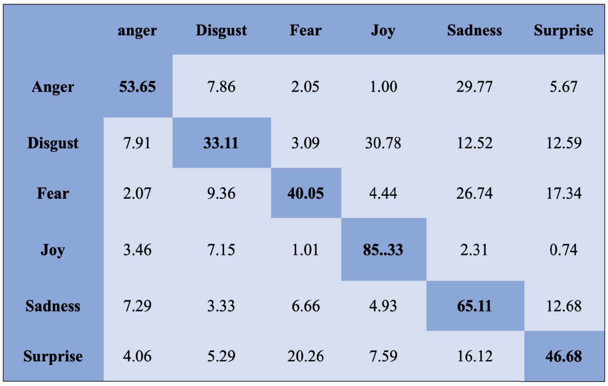

	anger	Disgust	Fear	Joy	Sadness	Surprise
Anger	53.65	7.86	2.05	1.00	29.77	5.67
Disgust	7.91	33.11	3.09	30.78	12.52	12.59
Fear	2.07	9.36	40.05	4.44	26.74	17.34
Joy	3.46	7.15	1.01	85..33	2.31	0.74
Sadness	7.29	3.33	6.66	4.93	65.11	12.68
Surprise	4.06	5.29	20.26	7.59	16.12	46.68

FIGURE 10. The confusion matrix of SD experiments on BAUM-1s dataset of augmented Mel spectrogram.

of 75.99%. Model B achieved average accuracy with the BAUM-1s dataset of the raw audio dataset is 40.57% for SD experiments. Model B achieved average accuracy with the BAUM-1s dataset of the augmented Mel spectrogram is 53.98% for SD experiments, as illustrated in Figure 10.

Validation accuracy is an important metric for assessing the generalization performance of a training model. The optimal model will be there when the validation accuracy of Model A and Model B achieves its maximum during the training process. The proposed study selects the best predictive model to minimize overfitting. The prediction performance of Model A and Model B improves as validation accuracy decreases. Overfitting occurs when the accuracy of validation decreases while training continuously increases. So, the training process will be early stopping. Avoiding overtraining and improving the model's performance can be achieved by early stopping. To achieve the highest classification performance, we evaluated validation accuracy in our experiments. When validation accuracy in training no longer increases, the model will have higher prediction accuracy.

B. SPEAKER-INDEPENDENT (SI) EXPERIMENTS

SI experiments were conducted using the same approach as SD experiments. However, the distribution of the dataset for IEMOCAP was different for SI experiments. The data were divided into two groups for the SI experiment depending on the subject. Since the utterance of emotions from the selected database was performed by twelve speakers, data from nine subjects was selected as the training sample, and data from the other three subjects was selected as the testing sample. The suggested model fitted the experimental data and has better predictive performance. The obtained results for SI experiments are shown in Figs. 11–15 to analyze the individual emotional groups' identification accuracy. Model B achieved average accuracy with the SAVEE and IEMOCAP databases at 96.85% and 88.80%, respectively, with augmented Mel spectrograms for SI experiments. While with raw data, the obtained accuracy is 87.54% and 69.53%, respectively. The best-fitted and predictive models are recorded when the proposed model achieves the highest validation accuracy during training. Therefore, the suggested model is more accurate at fitting the experimental data and has higher classification accuracy. Figure 11 shows the average accuracy achieved by Model B with the SAVEE database is 87.54%. The SAVEE database contains seven emotion categories, four of which, "anger", "sad", "surprise," and frustration, were identified with accuracies of 100%, 99.56%, 98.32%, and 98.28%, respectively, by the Model B with augmented

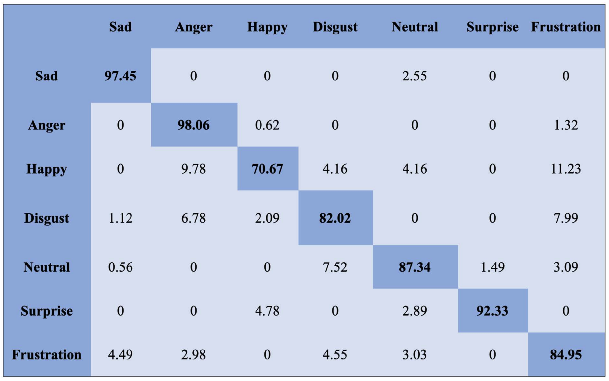

	Sad	Anger	Happy	Disgust	Neutral	Surprise	Frustration
Sad	97.45	0	0	0	2.55	0	0
Anger	0	98.06	0.62	0	0	0	1.32
Happy	0	9.78	70.67	4.16	4.16	0	11.23
Disgust	1.12	6.78	2.09	82.02	0	0	7.99
Neutral	0.56	0	0	7.52	87.34	1.49	3.09
Surprise	0	0	4.78	0	2.89	92.33	0
Frustration	4.49	2.98	0	4.55	3.03	0	84.95

FIGURE 11. The confusion matrix of SI experiments on SAVEE dataset of raw audio dataset.

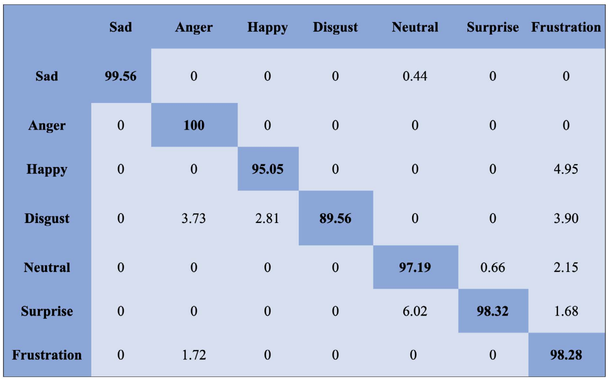

	Sad	Anger	Happy	Disgust	Neutral	Surprise	Frustration
Sad	99.56	0	0	0	0.44	0	0
Anger	0	100	0	0	0	0	0
Happy	0	0	95.05	0	0	0	4.95
Disgust	0	3.73	2.81	89.56	0	0	3.90
Neutral	0	0	0	0	97.19	0.66	2.15
Surprise	0	0	0	0	6.02	98.32	1.68
Frustration	0	1.72	0	0	0	0	98.28

FIGURE 12. The confusion matrix of SI experiments on SAVEE dataset of augmented Mel spectrogram.

Mel spectrogram as shown in Figure 12. In contrast, the other three emotions were identified with less than 98.00% accuracy, as represented in Figure 12. Model B achieved an average accuracy with the IEMOCAP database of 88.80%. Figure 13 shows that the IEMOCAP database, "anger," "sad," and "excited" were recognized with accuracies of 96.73%, 99.52%, and 93.22%, respectively, by the Model B with an augmented spectrogram. As shown in Figure 14, Model B recognized "sad" and "neutral" with the highest accuracies of 99.02% and 96.38% with the IEMOCAP dataset. Model B achieved average accuracy with the BAUM-1s dataset of the augmented Mel spectrogram of 48.67% for SI experiments.

C. RECOGNITION ACCURACY COMPARISON

Table 5 shows that the Model-A can learn emotional characteristics from raw audio samples to identify speech emotions. Furthermore, compared to Model-A, Model-B has significant advantages. The obtained average recognition and validation accuracy with the augmented Mel spectrogram are higher than the obtained accuracy from raw data. Model B achieved the best validation accuracy with fewer epochs and converged quicker than Model A. The proposed Model B performed adequately compared to other feature extraction and techniques. Also, Model-B is quicker in convergence than Model-A.

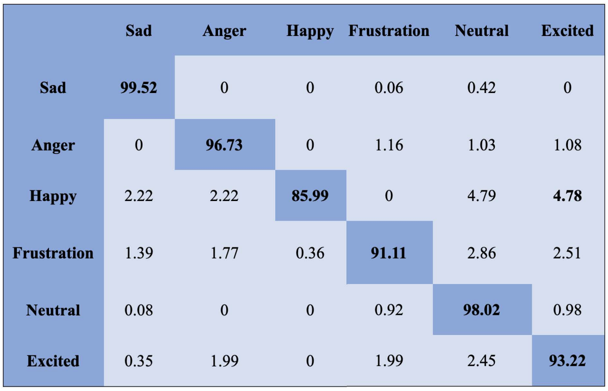

	Sad	Anger	Happy	Frustration	Neutral	Excited
Sad	99.52	0	0	0.06	0.42	0
Anger	0	96.73	0	1.16	1.03	1.08
Happy	2.22	2.22	85.99	0	4.79	**4.78**
Frustration	1.39	1.77	0.36	91.11	2.86	2.51
Neutral	0.08	0	0	0.92	98.02	0.98
Excited	0.35	1.99	0	1.99	2.45	93.22

FIGURE 13. The confusion matrix of SI experiments on IEMOCAP dataset of raw audio data.

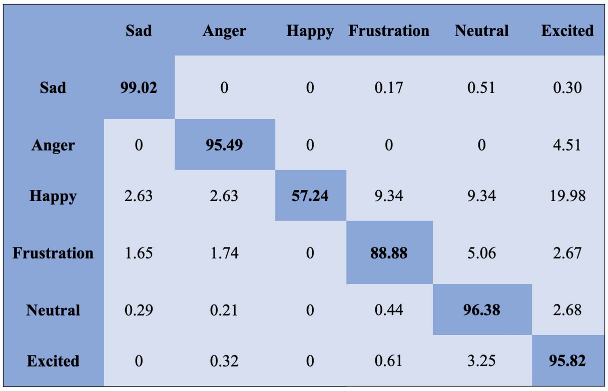

	Sad	Anger	Happy	Frustration	Neutral	Excited
Sad	99.02	0	0	0.17	0.51	0.30
Anger	0	95.49	0	0	0	4.51
Happy	2.63	2.63	57.24	9.34	9.34	19.98
Frustration	1.65	1.74	0	88.88	5.06	2.67
Neutral	0.29	0.21	0	0.44	96.38	2.68
Excited	0	0.32	0	0.61	3.25	95.82

FIGURE 14. The confusion matrix of SI experiments on IEMOCAP dataset of augmented Mel spectrogram.

Table 6 compares the average accuracy of the proposed Model B with the augmented Mel spectrogram of the SAVEE dataset with state-of-the-art approaches. Table 7 illustrates the average accuracy of the proposed Model B with an augmented Mel spectrogram of the IEMOCAP database with state-of-the-art approaches. Table 8 illustrates the average accuracy of the proposed Model B with an augmented Mel spectrogram of the proposed Model B BAUM-1s database with state-of-art approaches. Finally, Table 9 illustrates the Mid Mel spectrogram accuracy for three datasets. The mid-level Mel spectrogram possessed more than 75% accuracy for speaker-dependent experiments for SAVEE and IEMOCAP datasets. On the other hand, on the BAUM-1s dataset, the mid-level spectrogram achieved 42.40% and 36.88% accuracy for speaker-dependent and independent speaker experiments, respectively, which is slightly lower than the combined data augmentation approach.

D. DISCUSSION

Model A and Model B are comprised of five LFLBs and two LSTM layers to learn local level features and global level features. Because speech signals are time-varying signals and require complex evaluation to analyze time-varying features, the CNN+LSTM approach is proposed to recognize emotional states. Although this study has successfully acquired

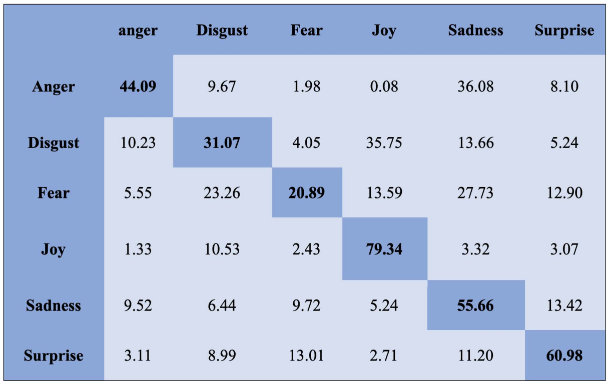

	anger	Disgust	Fear	Joy	Sadness	Surprise
Anger	**44.09**	9.67	1.98	0.08	36.08	8.10
Disgust	10.23	**31.07**	4.05	35.75	13.66	5.24
Fear	5.55	23.26	**20.89**	13.59	27.73	12.90
Joy	1.33	10.53	2.43	**79.34**	3.32	3.07
Sadness	9.52	6.44	9.72	5.24	**55.66**	13.42
Surprise	3.11	8.99	13.01	2.71	11.20	**60.98**

FIGURE 15. The confusion matrix of SI experiments on BAUM-1s dataset of augmented Mel spectrogram.

more emotional states from testing results, it is still important to investigate the possible correlation between performed emotions and auditory features. However, after learning several temporal features and emotions in experiments, our models could identify them with high accuracy. Furthermore, the proposed networks with comparable prediction results in extended trials demonstrate effective techniques for identifying speech emotions.

E. BLACK BOX

In the past few years, experts have started to investigate the ''black box'' issue to understand what is going on inside. Google researchers developed a new approach for the image classification model in 2015 to determine which features are utilized for classification. During the same year, researchers from the University of Wyoming identified how specific images might deceive a system by evaluating DNNs. A software engineer and a neurologist proposed the ''information bottleneck'' in 2017 [95]. Lehigh University developed DeepXplore to analyze neural networks by evaluating millions of neurons [96]. Stanford University [97] introduced ReluPlex based on mathematical arguments to validate the features of DNNs. Although these methods have taken a significant step in image classification, it is still not a universal answer to the ''black box'' issue [98], [99]. Additionally, we have studied significantly to understand better the developed DNNs employed to evaluate the speech. In the proposed study, we determine the impact of fundamental parameters of the proposed networks on classification results, and multiple models with changing layers and filters are counted at every layer. Also, we discover whether handmade features are effective in recognizing emotions; tests are performed on numerous handcrafted parameters. These attempts have allowed us to disclose additional information about the DNN in the experiments.

V. CONCLUSION

We proposed a new SER approach for semi-natural and spontaneous databases with an augmented Mel spectrogram. The suggested approach is used to generate suitable inputs for the 1D (Model A) and 2D (Model B) CNN+LSTM framework from an original audio dataset and develop appropriate deep models for feature learning. The proposed method learns local and global features from raw data and augmented Mel spectrogram. We used five LFLB blocks to extract local-level features from inputted data. Local features are inputted into the LSTM layer to understand contextual correlations. Moreover, features extracted by proposed models consist of local and long-term contextual dependency.

The overall performance of the proposed approach was analyzed on spontaneous and semi-natural databases. We noted that Model A and B extract discriminative features and represent high-level abstractions of speech datasets. The proposed approach showed that the overall accuracies of Model B are higher than other feature extraction and state-of-the-art approaches. However, the DNNs discussed in this study have improved their performance in speech emotion detection. However, several areas still need to be addressed. First, the mechanism by which the proposed networks identify emotions can not be fully described. The ''Black box'' of both models has not been investigated. However, most studies focused on the deep learning techniques employed in image processing. Speech is distinct from images; elucidating the ''BlackBox'' of deep networks optimizing speech processing requires extensive research. Secondly, achieving better accuracy in SER is not the final goal. A novel approach capable of learning more specific features or training a more accurate prediction model must be investigated. Finally, to maximize the advantages of different extracted features, create a mechanism for combining different deep features acquired by different deep learning models.

REFERENCES

[1] R. Li, Z. Wu, J. Jia, J. Li, W. Chen, and H. Meng, ''Inferring user emotive state changes in realistic human-computer conversational dialogs,'' in *Proc. 26th ACM Int. Conf. Multimedia (MM)*. New York, NY, USA: Association for Computing Machinery, Oct. 2018, pp. 136–144, doi: 10.1145/3240508.3240575.

[2] L. Khan, A. Amjad, K. M. Afaq, and H.-T. Chang, ''Deep sentiment analysis using CNN-LSTM architecture of English and Roman Urdu text shared in social media,'' *Appl. Sci.*, vol. 12, no. 5, p. 2694, Mar. 2022. [Online]. Available: https://www.mdpi.com/2076-3417/12/5/2694

[3] M. Farooq, F. Hussain, N. K. Baloch, F. R. Raja, H. Yu, and Y. B. Zikria, ''Impact of feature selection algorithm on speech emotion recognition using deep convolutional neural network,'' *Sensors*, vol. 20, no. 21, p. 6008, Oct. 2020. [Online]. Available: https://www.mdpi.com/1424-8220/20/21/6008

[4] L. Yi and M.-W. Mak, ''Adversarial data augmentation network for speech emotion recognition,'' in *Proc. Asia–Pacific Signal Inf. Process. Assoc. Annu. Summit Conf. (APSIPA ASC)*, Nov. 2019, pp. 529–534.

[5] F. Burkhardt, A. Paeschke, M. Rolfes, W. F. Sendlmeier, and B. Weiss, ''A database of German emotional speech,'' in *Proc. Interspeech, 9th Eur. Conf. Speech Commun. Technol. (Eurospeech)*. Lisbon, Portugal: ISCA, Sep. 2005, pp. 1517–1520. [Online]. Available: http://www.isca-speech.org/archive/interspeech_2005/i05_1517.html

[6] M. Sajjad and S. Kwon, ''Clustering-based speech emotion recognition by incorporating learned features and deep BiLSTM,'' *IEEE Access*, vol. 8, pp. 79861–79875, 2020.

[7] P. Song, ''Transfer linear subspace learning for cross-corpus speech emotion recognition,'' *IEEE Trans. Affect. Comput.*, vol. 10, no. 2, pp. 265–275, Apr. 2019.

[8] X. Zhao and S. Zhang, "Spoken emotion recognition via locality-constrained kernel sparse representation," *Neural Comput. Appl.*, vol. 26, no. 3, pp. 735–744, Apr. 2015, doi: 10.1007/s00521-014-1755-1.

[9] Z. Zixing, E. Coutinho, D. Jun, and B. Schuller, "Cooperative learning and its application to emotion recognition from speech," *IEEE/ACM Trans. Audio, Speech, Language Process.*, vol. 23, no. 1, pp. 115–126, Jan. 2015.

[10] M. Kayaoglu and C. E. Erdem, "Affect recognition using key frame selection based on minimum sparse reconstruction," in *Proc. ACM Int. Conf. Multimodal Interact. (ICMI)*. New York, NY, USA: Association for Computing Machinery, Nov. 2015, pp. 519–524, doi: 10.1145/2818346.2830594.

[11] B. Schuller, S. Steidl, A. Batliner, A. Vinciarelli, K. Scherer, F. Ringeval, M. Chetouani, F. Weninger, F. Eyben, E. Marchi, M. Mortillaro, H. Salamin, A. Polychroniou, F. Valente, and S. Kim, "The INTERSPEECH 2013 computational paralinguistics challenge: Social signals, conflict, emotion, autism," in *Proc. Interspeech*, Aug. 2013, pp. 148–152.

[12] M. Valstar, B. Schuller, K. Smith, F. Eyben, B. Jiang, S. Bilakhia, S. Schnieder, R. Cowie, and M. Pantic, "AVEC 2013: The continuous audio/visual emotion and depression recognition challenge," in *Proc. 3rd ACM Int. Workshop Audio/Visual Emotion Challenge (AVEC)*. New York, NY, USA: Association for Computing Machinery, Oct. 2013, pp. 3–10, doi: 10.1145/2512530.2512533.

[13] F. Eyben, K. R. Scherer, B. W. Schuller, J. Sundberg, E. André, C. Busso, L. Y. Devillers, J. Epps, P. Laukka, S. S. Narayanan, and K. P. Truong, "The Geneva minimalistic acoustic parameter set (GeMAPS) for voice research and affective computing," *IEEE Trans. Affect. Comput.*, vol. 7, no. 2, pp. 190–202, Apr./Jun. 2016.

[14] S. Zhang, X. Zhao, and Q. Tian, "Spontaneous speech emotion recognition using multiscale deep convolutional LSTM," *IEEE Trans. Affect. Comput.*, early access, Oct. 17, 2019, doi: 10.1109/TAFFC.2019.2947464.

[15] S. Zhang, A. Chen, W. Guo, Y. Cui, X. Zhao, and L. Liu, "Learning deep binaural representations with deep convolutional neural networks for spontaneous speech emotion recognition," *IEEE Access*, vol. 8, pp. 23496–23505, 2020.

[16] A. Amjad, L. Khan, and H.-T. Chang, "Effect on speech emotion classification of a feature selection approach using a convolutional neural network," *PeerJ Comput. Sci.*, vol. 7, p. e766, Nov. 2021, doi: 10.7717/peerj-cs.766.

[17] M. El Ayadi, M. S. Kamel, and F. Karray, "Survey on speech emotion recognition: Features, classification schemes, and databases," *Pattern Recognit.*, vol. 44, no. 3, pp. 572–587, 2011. [Online]. Available: https://www.sciencedirect.com/science/article/pii/S0031320310004619

[18] L. Chen, X. Mao, Y. Xue, and L. L. Cheng, "Speech emotion recognition: Features and classification models," *Digit. Signal Process.*, vol. 22, no. 6, pp. 1154–1160, Dec. 2012. [Online]. Available: https://www.sciencedirect.com/science/article/pii/S1051200412001133

[19] G. E. Hinton and R. R. Salakhutdinov, "Reducing the dimensionality of data with neural networks," *Science*, vol. 313, no. 5786, pp. 504–507, 2006. [Online]. Available: https://www.science.org/doi/abs/10.1126/science.1127647

[20] J. Zhao, X. Mao, and L. Chen, "Speech emotion recognition using deep 1D & 2D CNN LSTM networks," *Biomed. Signal Process. Control*, vol. 47, pp. 312–323, 2019. [Online]. Available: https://www.sciencedirect.com/science/article/pii/S1746809418302337

[21] M. Lech, M. Stolar, C. Best, and R. Bolia, "Real-time speech emotion recognition using a pre-trained image classification network: Effects of bandwidth reduction and companding," *Frontiers Comput. Sci.*, vol. 2, p. 14, May 2020. [Online]. Available: https://www.frontiersin.org/article/10.3389/fcomp.2020.00014

[22] B. J. Abbaschian, D. Sierra-Sosa, and A. Elmaghraby, "Deep learning techniques for speech emotion recognition, from databases to models," *Sensors*, vol. 21, no. 4, p. 1249, Feb. 2021, doi: 10.3390/s21041249.

[23] C.-H. Wu, H.-T. Chang, and A. Amjad, "Eye in-painting using WGAN-GP for face images with mosaic," *Proc. SPIE*, vol. 11584, pp. 146–149, Nov. 2020, doi: 10.1117/12.2580635.

[24] L. Khan, A. Amjad, N. Ashraf, H.-T. Chang, and A. Gelbukh, "Urdu sentiment analysis with deep learning methods," *IEEE Access*, vol. 9, pp. 97803–97812, 2021.

[25] A. Amjad, L. Khan, and H.-T. Chang, "Semi-natural and spontaneous speech recognition using deep neural networks with hybrid features unification," *Processes*, vol. 9, no. 12, p. 2286, Dec. 2021. [Online]. Available: https://www.mdpi.com/2227-9717/9/12/2286

[26] A. Krizhevsky, I. Sutskever, and G. E. Hinton, "ImageNet classification with deep convolutional neural networks," *Commun. ACM*, vol. 60, no. 6, pp. 84–90, May 2017, doi: 10.1145/3065386.

[27] A. Graves, "Supervised sequence labelling," in *Supervised Sequence Labelling with Recurrent Neural Networks*. Berlin, Germany: Springer, 2012, pp. 5–13, doi: 10.1007/978-3-642-24797-2_2.

[28] R. E. Harper, T. Rodden, Y. Rogers, and A. Sellen, *Human-Computer Interaction in the year 2020*. 2008. [Online]. Available: https://www.microsoft.com/en-us/research/publication/being-human-human-computer-interaction-in-the-year-2020/

[29] B. Schuller, S. Steidl, A. Batliner, A. Vinciarelli, K. Scherer, F. Ringeval, M. Chetouani, F. Weninger, F. Eyben, E. Marchi, M. Mortillaro, H. Salamin, A. Polychroniou, F. Valente, and S. Kim, "The INTERSPEECH 2013 computational paralinguistics challenge: Social signals, conflict, emotion, autism," in *Proc. Interspeech, 14th Annu. Conf. Int. Speech Commun. Assoc.*, Lyon, France, Aug. 2013, pp. 1–5. [Online]. Available: https://hal.sorbonne-universite.fr/hal-02423147

[30] A. Stuhlsatz, C. Meyer, F. Eyben, T. Zielke, G. Meier, and B. Schuller, "Deep neural networks for acoustic emotion recognition: Raising the benchmarks," in *Proc. IEEE Int. Conf. Acoust., Speech Signal Process. (ICASSP)*, May 2011, pp. 5688–5691.

[31] K. Han, D. Yu, and I. Tashev, "Speech emotion recognition using deep neural network and extreme learning machine," in *Proc. Interspeech*, Sep. 2014, pp. 1–5.

[32] Q. Mao, M. Dong, Z. Huang, and Y. Zhan, "Learning salient features for speech emotion recognition using convolutional neural networks," *IEEE Trans. Multimedia*, vol. 16, no. 8, pp. 2203–2213, Dec. 2014.

[33] G. Trigeorgis, F. Ringeval, R. Brueckner, E. Marchi, M. A. Nicolaou, B. Schuller, and S. Zafeiriou, "Adieu features? End-to-end speech emotion recognition using a deep convolutional recurrent network," in *Proc. IEEE Int. Conf. Acoust., Speech Signal Process. (ICASSP)*, Mar. 2016, pp. 5200–5204.

[34] C.-W. Huang and S. S. Narayanan, "Deep convolutional recurrent neural network with attention mechanism for robust speech emotion recognition," in *Proc. IEEE Int. Conf. Multimedia Expo (ICME)*, Jul. 2017, pp. 583–588.

[35] K. Han, D. Yu, and I. Tashev, "Speech emotion recognition using deep neural network and extreme learning machine," in *Proc. Interspeech*, Sep. 2014, pp. 223–227.

[36] Z.-Q. Wang and I. Tashev, "Learning utterance-level representations for speech emotion and age/gender recognition using deep neural networks," in *Proc. IEEE Int. Conf. Acoust., Speech Signal Process. (ICASSP)*, Mar. 2017, pp. 5150–5154.

[37] A. M. Badshah, B. N. Rahim, N. Ullah, J. Ahmad, K. Muhammad, M. Y. Lee, S. Kwon, and S. W. Baik, "Deep features-based speech emotion recognition for smart affective services," *Multimedia Tools Appl.*, vol. 78, no. 5, pp. 5571–5589, Mar. 2019, doi: 10.1007/s11042-017-5292-7.

[38] S. Zhang, S. Zhang, T. Huang, W. Gao, and Q. Tian, "Learning affective features with a hybrid deep model for audio–visual emotion recognition," *IEEE Trans. Circuits Syst. Video Technol.*, vol. 28, no. 10, pp. 3030–3043, Oct. 2018.

[39] Z. Zhao, Z. Bao, Y. Zhao, Z. Zhang, N. Cummins, Z. Ren, and B. Schuller, "Exploring deep spectrum representations via attention-based recurrent and convolutional neural networks for speech emotion recognition," *IEEE Access*, vol. 7, pp. 97515–97525, 2019.

[40] Z. Zhao, Y. Zhao, Z. Bao, H. Wang, Z. Zhang, and C. Li, "Deep spectrum feature representations for speech emotion recognition," in *Proc. Joint Workshop 4th Workshop Affect. Social Multimedia Comput. 1st Multi-Modal Affect. Comput. Large-Scale Multimedia Data*. New York, NY, USA: Association for Computing Machinery, Oct. 2018, pp. 27–33, doi: 10.1145/3267935.3267948.

[41] I. Ameer, N. Ashraf, G. Sidorov, and H. Gómez Adorno, "Multi-label emotion classification using content-based features in Twitter," *Computación y Sistemas*, vol. 24, no. 3, pp. 1159–1164, Sep. 2020.

[42] N. Ashraf, A. Zubiaga, and A. Gelbukh, "Abusive language detection in YouTube comments leveraging replies as conversational context," *PeerJ Comput. Sci.*, vol. 7, p. e742, Oct. 2021.

[43] N. Ashraf, R. Mustafa, G. Sidorov, and A. Gelbukh, "Individual vs. group violent threats classification in online discussions," in *Proc. Companion Proc. Web Conf.*, Apr. 2020, pp. 629–633.

[44] A. Mateen, A. Khalid, L. Khan, S. Majeed, and T. Akhtar, "Vigorous algorithms to control urban vehicle traffic," in *Proc. IEEE/ACIS 15th Int. Conf. Comput. Inf. Sci. (ICIS)*, Jun. 2016, pp. 1–5.

[45] M. Ashraf, L. Khan, M. Tahir, A. Alghamdi, M. Alqarni, T. Sabbah, and M. Khan, "A study on usability awareness in local IT industry," *Int. J. Adv. Comput. Sci. Appl.*, vol. 9, no. 5, pp. 427–432, 2018.

[46] H. M. Fayek, M. Lech, and L. Cavedon, "Evaluating deep learning architectures for speech emotion recognition," *Neural Netw.*, vol. 92, pp. 60–68, Aug. 2017. [Online]. Available: https://www.sciencedirect.com/science/article/pii/S089360801730059X

[47] S. Hochreiter and J. Schmidhuber, "Long short-term memory," *Neural Comput.*, vol. 9, no. 8, pp. 1735–1780, Nov. 1997, doi: 10.1162/neco.1997.9.8.1735.

[48] T. M. Wani, T. S. Gunawan, S. A. A. Qadri, H. Mansor, M. Kartiwi, and N. Ismail, "Speech emotion recognition using convolution neural networks and deep stride convolutional neural networks," in *Proc. 6th Int. Conf. Wireless Telematics (ICWT)*, Sep. 2020, pp. 1–6.

[49] G. Bertasius, J. Shi, and L. Torresani, "DeepEdge: A multi-scale bifurcated deep network for top-down contour detection," *CoRR*, vol. abs/1412.1123, pp. 1–10, Dec. 2014.

[50] Z. Cai, Q. Fan, R. S. Feris, and N. Vasconcelos, "A unified multi-scale deep convolutional neural network for fast object detection," *CoRR*, vol. abs/1607.07155, pp. 1–16, Jul. 2016.

[51] S. Zhalehpour, O. Onder, Z. Akhtar, and C. E. Erdem, "BAUM-1: A spontaneous audio-visual face database of affective and mental states," *IEEE Trans. Affect. Comput.*, vol. 8, no. 3, pp. 300–313, Jul./Sep. 2016.

[52] A. B. Kandali, A. Routray, and T. K. Basu, "Emotion recognition from assamese speeches using MFCC features and GMM classifier," in *Proc. TENCON IEEE Region 10 Conf.*, Nov. 2008, pp. 1–5.

[53] V. B. Waghmare, R. Deshmukh, P. Shrishrimal, G. Janvale, and B. Ambedkar, "Emotion recognition system from artificial Marathi speech using MFCC and LDA techniques," in *Proc. Int. Conf. Adv. Commun., Netw., Comput.*, 2014, pp. 1–9.

[54] M. S. Likitha, S. R. R. Gupta, K. Hasitha, and A. U. Raju, "Speech based human emotion recognition using MFCC," in *Proc. Int. Conf. Wireless Commun., Signal Process. Netw. (WiSPNET)*, Mar. 2017, pp. 2257–2260.

[55] F. Chenchah and Z. Lachiri, "Acoustic emotion recognition using linear and nonlinear cepstral coefficients," *Int. J. Adv. Comput. Sci. Appl.*, vol. 6, no. 11, pp. 1–4, 2015, doi: 10.14569/IJACSA.2015.061119.

[56] N. J. Nalini, S. Palanivel and M. Balasubramanian, "Speech emotion recognition using residual phase and MFCC features," *Int. J. Eng. Technol.*, vol. 5, no. 6, pp. 4515–4527, 2013.

[57] N. J. Nalini and S. Palanivel, "Music emotion recognition: The combined evidence of MFCC and residual phase," *Egyptian Informat. J.*, vol. 17, no. 1, pp. 1–10, Mar. 2016. [Online]. Available: https://www.sciencedirect.com/science/article/pii/S1110866515000419

[58] E. M. Schmidt, J. J. Scott, and Y. E. Kim, "Feature learning in dynamic environments: Modeling the acoustic structure of musical emotion," in *Proc. ISMIR*, 2012, pp. 1–6.

[59] D. Le and E. M. Provost, "Emotion recognition from spontaneous speech using hidden Markov models with deep belief networks," in *Proc. IEEE Workshop Autom. Speech Recognit. Understand.*, Dec. 2013, pp. 216–221.

[60] G. Almpanidis and C. Kotropoulos, "Phonemic segmentation using the generalised gamma distribution and small sample Bayesian information criterion," *Speech Commun.*, vol. 50, no. 1, pp. 38–55, Jan. 2008. [Online]. Available: https://www.sciencedirect.com/science/article/pii/S0167639307001197

[61] W. Q. Zheng, J. S. Yu, and Y. X. Zou, "An experimental study of speech emotion recognition based on deep convolutional neural networks," in *Proc. Int. Conf. Affect. Comput. Intell. Interact. (ACII)*, Sep. 2015, pp. 827–831.

[62] S. Yoon, S. Byun, and K. Jung, "Multimodal speech emotion recognition using audio and text," in *Proc. IEEE Spoken Lang. Technol. Workshop (SLT)*, Dec. 2018, pp. 112–118.

[63] R. Singh, H. Puri, N. Aggarwal, and V. Gupta, "An efficient language-independent acoustic emotion classification system," *Arabian J. Sci. Eng.*, vol. 45, no. 4, pp. 3111–3121, Apr. 2020, doi: 10.1007/s13369-019-04293-9.

[64] H. Meng, T. Yan, F. Yuan, and H. Wei, "Speech emotion recognition from 3D log-mel spectrograms with deep learning network," *IEEE Access*, vol. 7, pp. 125868–125881, 2019.

[65] T. Anvarjon, Mustaqeem, and S. Kwon, "Deep-Net: A lightweight CNN-based speech emotion recognition system using deep frequency features," *Sensors*, vol. 20, no. 18, p. 5212, Sep. 2020. [Online]. Available: https://www.mdpi.com/1424-8220/20/18/5212

[66] B. Zhang, E. M. Provost, and G. Essi, "Cross-corpus acoustic emotion recognition from singing and speaking: A multi-task learning approach," in *Proc. IEEE Int. Conf. Acoust., Speech Signal Process. (ICASSP)*, Mar. 2016, pp. 5805–5809.

[67] P. Nantasri, E. Phaisangittisagul, J. Karnjana, S. Boonkla, S. Keerativittayanun, A. Rugchatjaroen, S. Usanavasin, and T. Shinozaki, "A light-weight artificial neural network for speech emotion recognition using average values of MFCCs and their derivatives," in *Proc. 17th Int. Conf. Electr. Eng./Electron., Comput., Telecommun. Inf. Technol. (ECTI-CON)*, Jun. 2020, pp. 41–44.

[68] A. M. Badshah, J. Ahmad, N. Rahim, and S. W. Baik, "Speech emotion recognition from spectrograms with deep convolutional neural network," in *Proc. Int. Conf. Platform Technol. Service (PlatCon)*, Feb. 2017, pp. 1–5.

[69] A. Krizhevsky, I. Sutskever, and G. E. Hinton, "ImageNet classification with deep convolutional neural networks," in *Advances in Neural Information Processing Systems*, vol. 25, F. Pereira, C. J. C. Burges, L. Bottou, and K. Q. Weinberger, Eds. Red Hook, NY, USA: Curran Associates, 2012. [Online]. Available: https://proceedings.neurips.cc/paper/2012/file/c399862d3b9d6b76c8436e924a68c45b-Paper.pdf

[70] A. Bhavan, P. Chauhan, Hitkul, and R. R. Shah, "Bagged support vector machines for emotion recognition from speech," *Knowl.-Based Syst.*, vol. 184, Nov. 2019, Art. no. 104886. [Online]. Available: https://www.sciencedirect.com/science/article/pii/S0950705119303533

[71] K. Zvarevashe and O. Olugbara, "Ensemble learning of hybrid acoustic features for speech emotion recognition," *Algorithms*, vol. 13, no. 3, p. 70, Mar. 2020. [Online]. Available: https://www.mdpi.com/1999-4893/13/3/70

[72] C. Zheng, C. Wang, and N. Jia, "An ensemble model for multi-level speech emotion recognition," *Appl. Sci.*, vol. 10, no. 1, p. 205, Dec. 2019. [Online]. Available: https://www.mdpi.com/2076-3417/10/1/205

[73] Y. Kim, H. Lee, and E. M. Provost, "Deep learning for robust feature generation in audiovisual emotion recognition," in *Proc. IEEE Int. Conf. Acoust., Speech Signal Process.*, May 2013, pp. 3687–3691.

[74] Z. Huang, M. Dong, Q. Mao, and Y. Zhan, "Speech emotion recognition using CNN," in *Proc. 22nd ACM Int. Conf. Multimedia (MM)*. New York, NY, USA: Association for Computing Machinery, Nov. 2014, pp. 801–804, doi: 10.1145/2647868.2654984.

[75] S. Demircan and H. Kahramanli, "Application of fuzzy C-means clustering algorithm to spectral features for emotion classification from speech," *Neural Comput. Appl.*, vol. 29, no. 8, pp. 59–66, Apr. 2018.

[76] E. M. Provost, "Identifying salient sub-utterance emotion dynamics using flexible units and estimates of affective flow," in *Proc. IEEE Int. Conf. Acoust., Speech Signal Process.*, May 2013, pp. 3682–3686.

[77] Y. LeCun, B. Boser, J. S. Denker, D. Henderson, R. E. Howard, W. Hubbard, and L. D. Jackel, "Backpropagation applied to handwritten zip code recognition," *Neural Comput.*, vol. 1, no. 4, pp. 541–551, 1989.

[78] B. Boser, E. Sackinger, J. Bromley, Y. LeCun, R. Howard, and L. Jackel, "An analog neural network processor and its application to high-speed character recognition," in *Proc. Int. Joint Conf. Neural Netw. (IJCNN-Seattle)*, vol. 1, 1991, pp. 415–420.

[79] S. Behnke, "Discovering hierarchical speech features using convolutional non-negative matrix factorization," in *Proc. Int. Joint Conf. Neural Netw.*, vol. 4, 2003, pp. 2758–2763.

[80] S. Ioffe and C. Szegedy, "Batch normalization: Accelerating deep network training by reducing internal covariate shift," in *Proc. 32nd Int. Conf. Mach. Learn.*, vol. 37, F. Bach and D. Blei, Eds. Lille, France: PMLR, Jul. 2015, pp. 448–456. [Online]. Available: http://proceedings.mlr.press/v37/ioffe15.html

[81] S. Ioffe and C. Szegedy, "Batch normalization: Accelerating deep network training by reducing internal covariate shift," *CoRR*, vol. abs/1502.03167, pp. 1–11, Feb. 2015.

[82] D.-A. Clevert, T. Unterthiner, and S. Hochreiter, "Fast and accurate deep network learning by exponential linear units (ELUs)," 2015, *arXiv:1511.07289*.

[83] D. Ciresan, U. Meier, and J. Schmidhuber, "Multi-column deep neural networks for image classification," in *Proc. IEEE Conf. Comput. Vis. Pattern Recognit.*, Jun. 2012, pp. 3642–3649.

[84] F. Gers, J. Schmidhuber, and F. Cummins, "Learning to forget: Continual prediction with LSTM," in *Proc. 9th Int. Conf. Artif. Neural Netw. (ICANN)*, vol. 2, 1999, pp. 850–855.

[85] Y. Huang, A. Wu, G. Zhang, and Y. Li, "Speech emotion recognition based on Coiflet wavelet packet cepstral coefficients," in *Pattern Recognition*, S. Li, C. Liu, and Y. Wang, Eds. Berlin, Germany: Springer, 2014, pp. 436–443.

[86] S. Wu, T. H. Falk, and W.-Y. Chan, "Automatic speech emotion recognition using modulation spectral features," *Speech Commun.*, vol. 53, no. 5, pp. 768–785, 2011. [Online]. Available: https://www.sciencedirect.com/science/article/pii/S0167639310001470

[87] (2016). *GitHub—Keras-Team/Keras: Deep Learning for Humans*. [Online]. Available: https://github.com/keras-team/keras

[88] J. Bergstra, R. Bardenet, Y. Bengio, and B. Kégl, "Algorithms for hyper-parameter optimization," in *Proc. 24th Int. Conf. Neural Inf. Process. Syst. (NIPS)*. Red Hook, NY, USA: Curran Associates, 2011, pp. 2546–2554.

[89] J. Snoek, H. Larochelle, and R. P. Adams, "Practical Bayesian optimization of machine learning algorithms," in *Proc. Adv. Neural Inf. Process. Syst.*, 2012, pp. 1–9.

[90] J. Bergstra, D. Yamins, and D. D. Cox, "Hyperopt: A Python library for optimizing the hyperparameters of machine learning algorithms," in *Proc. 12th Python Sci. Conf.*, S. van der Walt, J. Millman, and K. Huff, Eds., 2013, pp. 13–19.

[91] K. Velusamy and R. Amalraj, "Cascade correlation neural network with deterministic weight modification for predicting stock market price," *IOP Conf. Ser., Mater. Sci. Eng.*, vol. 1110, no. 1, Mar. 2021, Art. no. 012005, doi: 10.1088/1757-899x/1110/1/012005.

[92] A. Neumaier, "Solving ill-conditioned and singular linear systems: A tutorial on regularization," *SIAM Rev.*, vol. 40, no. 3, pp. 636–666, 1998.

[93] R. Kohavi, "A study of cross-validation and bootstrap for accuracy estimation and model selection," *Ijcai*, vol. 14, no. 2, pp. 1137–1145, 1995.

[94] J. Loughrey and P. Cunningham, "Using early-stopping to avoid overfitting in wrapper-based feature selection employing stochastic search,"in *Proc. 10th U.K. Workshop Case-Based Reasoning*, 2005, pp. 3–10.

[95] N. Wolchover and L. Reading, "New theory cracks open the black box of deep learning," *Quanta Mag.*, vol. 3, 2017.

[96] K. Pei, Y. Cao, J. Yang, and S. Jana, "DeepXplore: Automated whitebox testing of deep learning systems," *CoRR*, vol. abs/1705.06640, pp. 1–18, May 2017.

[97] G. Katz, C. W. Barrett, D. L. Dill, K. Julian, and M. J. Kochenderfer, "Reluplex: An efficient SMT solver for verifying deep neural networks," *CoRR*, vol. abs/1702.01135, pp. 1–31, Feb. 2017.

[98] D. Castelvecchi, "Can we open the black box of AI?" *Nature*, vol. 538, no. 7623, pp. 20–23, Oct. 2016.

[99] MIT Technology Review. (2017). *The Dark Secret at the Heart of AI*. [Online]. Available: https://www.technologyreview.com/2017/04/11/5113/the-dark-secret-at-the-heart-of-ai/

AMMAR AMJAD received the master's degree in computer science from the National College of Business Administration and Economics, in March 2017. He is currently pursuing the Ph.D. degree in electrical engineering with the Division of Computer Science and Information Engineering, Chang Gung University, Taiwan. His research interests include speech processing, language learning, speech analysis, speech synthesis, voice pathologies, auditory neuroscience, and machine learning.

LAL KHAN was born in D G Khan, Punjab. He received the M.S. degree in computer science from the Federal Urdu University of Arts, Science and Technology, Islamabad, in 2017. He is currently a Ph.D. Scholar with the Department of Computer Science and Information Engineering, Chang Gung University, Taiwan. He is also working in NLP task for resource-deprived languages. His research interests include machine learning, deep learning, natural language processing (NLP), and speech recognition.

NOMAN ASHRAF received the Ph.D. degree from the Centro de Investigación en Computación, Instituto Politécnico Nacional (IPN). His specialization lies in natural language processing (NLP). His research interests include hate speech detection, depression detection, and emotion detection. He joined Mayo Clinic as a Research Scholar and currently working on several projects related to Breast Cancer (BC) Prediction from Social Media (SM) and Clinical Text Datasets. Before joining Mayo Clinic, he was working as a Machine Learning Engineer at International Consulting Associates, Inc.

MUHAMMAD BILAL MAHMOOD received the master's degree in computer engineering from the National University of Sciences and Technology, Islamabad, Pakistan, in 2015. He is currently a Ph.D. Scholar with the Department of Software Engineering, Dalia University of Technology, China. His research interests include natural language processing (NLP), the IoT, and cloud computing.

HSIEN-TSUNG CHANG received the M.S. and Ph.D. degrees from the Department of Computer Science and Information (CSIE), National Chung Cheng University, in July 2000 and July 2007, respectively. He joined the Faculty of Computer Science and the Information Engineering Department, Chang Gung University and worked as an Associate Professor. He is also a member of the Artificial Intelligence Research Center, Chang Gung University, and the Department of Physical Medicine and Rehabilitation, Chang Gung Memorial Hospital. His research interests include artificial intelligence, natural language processing, information retrieval, big data, web services, and search engines. He is the Director of the Web Information and Data Engineering Laboratory (WIDE Laboratory).